

Influence of an anomalous temperature-dependence of the phase coherence length on the conductivity of magnetic topological insulators

V. Tkáč,^{1,2} K. Výborný,³ V. Komanický,² J. Warmuth,⁴ M. Michiardi,⁵ A. S. Ngankeu,⁵ R. Tarasenko,^{1,2} M. Vališka,¹ V. Stetsovych,³ K. Carva,¹ I. Garate,⁶ M. Bianchi,⁵ J. Wiebe,⁴ V. Holý,¹ Ph. Hofmann,⁵ G. Springholz,⁷ V. Sechovský,¹ and J. Honolka³

¹*Department of Condensed Matter Physics, Faculty of Mathematics and Physics, Charles University, Ke Karlovu 5, CZ-12116 Prague 2, Czech Republic*

²*Institute of Physics, P. J. Šafárik University, Park Angelinum 9, 040 01 Košice, Slovak Republic*

³*Institute of Physics, Academy of Sciences of the Czech Republic, Na Slovance 2, CZ-18221 Prague 8, Czech Republic*

⁴*Department of Physics, University of Hamburg, D-20355 Hamburg, DE*

⁵*Department of Physics and Astronomy, Interdisciplinary Nanoscience Center (iNANO), University of Aarhus, 8000 Aarhus C, DK*

⁶*Département de physique and Institut quantique,*

Université de Sherbrooke, Sherbrooke (Québec) CA J1K 2R1

⁷*Institute of Semiconductor and Solid State Physics,*

Johannes Kepler University, Altenbergerstrasse 69, A-4040 Linz, Austria

(Dated: Apr10, 2018 - edited by KV)

Magnetotransport constitutes a useful probe to understand the interplay between electronic band topology and magnetism in spintronics devices based on topological materials. A recent theory of Lu and Shen [Phys. Rev. Lett. 112, 146601 (2014)] on magnetically doped topological insulators predicts that quantum corrections $\Delta\kappa$ to the temperature-dependence of the conductivity can change sign during the Curie transition. This phenomenon has been attributed to a suppression of the Berry phase of the topological surface states at the Fermi level, caused by a magnetic energy gap. Here, we demonstrate experimentally that $\Delta\kappa$ can reverse its sign even when the Berry phase at the Fermi level remains unchanged, provided that the inelastic scattering length decreases with temperature below the Curie transition.

The material class of topological insulators (TIs) comprises fascinating fundamental physics and offers potential for spintronic applications [1–3]. In three dimensions, prototype TI materials are bismuth chalcogenides, characterized by a single gapless topological surface state (TSS). This TSS, protected by time-reversal symmetry (TRS), has a Dirac-like linear energy dispersion and spin-momentum locking [4]. Consequently, an electron traveling around the Fermi circle of a TSS accrues a quantum (Berry) phase of π . In presence of disorder, this Berry phase ϕ_{Be} leads to an enhancement of the conductivity via quantum interference (QI). This effect manifests itself most clearly through a negative magnetoconductance, i.e. weak antilocalization (WAL). In spintronics applications, it is desirable to open an energy gap Δ in the TSS while minimising dopant-induced Coulomb disorder effects [5]. This can in principle be achieved by doping the TI with magnetic impurities, provided that the latter order ferromagnetically in the direction perpendicular to the surface. In such scenario, the Berry phase is suppressed and the magnetoconductance can change sign if the Fermi energy lies close to the gap edge, giving rise to weak localization (WL).

The WAL-to-WL crossover [6] has been experimentally observed in the magnetic field (B) dependence of the longitudinal conductivity σ_{xx} , for Mn-doped [7] Bi₂Se₃ and other magnetically doped TI thin films [8–10] in the ferromagnetic regime. However, a dilemma has emerged

concerning the quantum correction to the zero-field conductivity, $\Delta\sigma_{xx}(T, B = 0) = \kappa \ln T$. While it is expected that WAL-to-WL crossover should be accompanied by a change from $\kappa < 0$ to $\kappa > 0$, experiments show $\kappa > 0$ regardless of the concentration of magnetic impurities (positive κ is expected for an ordinary dirty metal under WL conditions). The theory by Lu and Shen (LS) [11] suggests to resolve this dilemma by taking into account 2D electron-electron interaction (EEI) contributions σ_{xx}^{ee} with $\kappa^{ee} > 0$, which in $\kappa = \kappa^{ee} + \kappa^{qi}$ prevail over the QI contribution κ^{qi} , but do not override the weak localisation signatures in $\sigma_{xx}(B)$ (here, the effect of B on κ^{ee} can be neglected as Fig. 4(d) in Ref. [11] implies). This theory not only closes the fundamental gap of understanding experimental data of $\sigma_{xx}(B)$ and $\sigma_{xx}(T)$ but offers a general procedure to identify the origin of gap Δ in TSSs. It relies on field dependent changes $\Delta\kappa(B) = \kappa(B) - \kappa(0) \propto \kappa^{qi}$ with opposite sign κ^{qi} for the WAL and WL phases.

In this work, we test the LS theory in the case of a magnetically doped TI (Mn-doped Bi₂Se₃), and demonstrate that it fails to correctly identify the reason for gap opening in this particular system and show what assumption of the LS theory needs to be modified in order to arrive at the right interpretation. We present field- and temperature-dependent data of longitudinal (σ_{xx}) and transverse (σ_{xy}) conductances in Mn-doped MBE-grown Bi₂Se₃ thin films ($x_{Mn} = 0 - 8\%$). The

data both above and below the ferromagnetic ordering temperature T_C is analysed in terms of QI and EEI effects [11, 12] and we observe a distinct transition from $\Delta\kappa(B = 5 \text{ T}) = +0.5 e^2/h$ at high temperatures to $\Delta\kappa(B = 5 \text{ T}) = -0.5 e^2/h$ below T_C in apparent agreement with predictions of the LS theory concerning the TRS breaking effect induced by ferromagnetic exchange field (H_z^{Ex}). This is, however, not what really happens in Mn-doped Bi_2Se_3 as we explain below. The LS theory as published [11] relies on the coherence length following $l_\Phi \propto T^{-p/2}$ with certain temperature-independent exponent p . While this assumption is fulfilled in many systems (in clean Bi_2Se_3 , we observe Nyquist-type scaling with $p = 1$ for example), our Mn-doped samples show an anomalous temperature dependence of l_Φ . A maximum appears close to $T = T_C$, which is clearly inconsistent with $l_\Phi \propto T^{-p/2}$ unless different exponents (of opposite sign) are taken in the paramagnetic ($T > T_C$) and ferromagnetic ($T < T_C$) phases. When this fact is taken into account, the sign change in $\Delta\kappa$ may be explained without invoking a change in the Berry phase of the TSS (i.e. with zero or negligible $\langle H_z^{\text{Ex}} \rangle$), in agreement with other experimental evidence such as ARPES (also explained below).

Mn-doped $\text{Bi}_2\text{Se}_3(0001)$ thin films were grown on $\text{BaF}_2(111)$ substrates using MBE with varying Mn concentrations up to the solubility limit of about 8 at. % [7, 13] as described in our previous works [14]. Film thicknesses t were chosen in the range $t = (20 - 40)$ nm, just above the thickness limit where top and bottom TSSs of Bi_2Se_3 slabs start to directly hybridize and develop a gap Δ_{hyb} [15–17].

For magnetotransport measurements we fabricated standard Hall-bars as sketched in Fig. 1(a) (see also Supporting Information) with longitudinal and transverse voltage probes to determine σ_{xx} and σ_{xy} . In Fig. 1(b) we show the temperature dependence of the electrical resistivity $\rho_{xx} = \sigma_{xx}^{-1}$ in zero magnetic field for $t = (40 \pm 5)$ nm films with Mn concentrations $x_{\text{Mn}} = 0\%$, 4%, and 8%. Resistivities are of the order of 1 m Ωcm , similar to those reported in the quantum transport literature [4]. Starting at high temperatures we generally observe a resistivity drop with decreasing temperature indicating metallic behavior, while below 30 K all samples exhibit a characteristic increase in resistivity, an effect which we will discuss in the framework of QI and EEIs.

Charge carrier densities n , mobilities μ as well as magnetic ordering temperatures T_c are derived from Hall measurements in the temperature range between 1.8 K and 40 K. The Hall resistance R_{xy} is given by $R_{xy}(B, T) = R_N B + R_A(B, T)$, where the linear contribution R_N corresponds to the normal Hall effect and R_A describes the magnetization dependent anomalous Hall effect (AHE). The results are given in Tab. I. All samples are n-type with carrier concentrations $n = 10^{18} - 10^{19} \text{ cm}^{-3}$ characteristic for heavily doped Bi_2Se_3 sam-

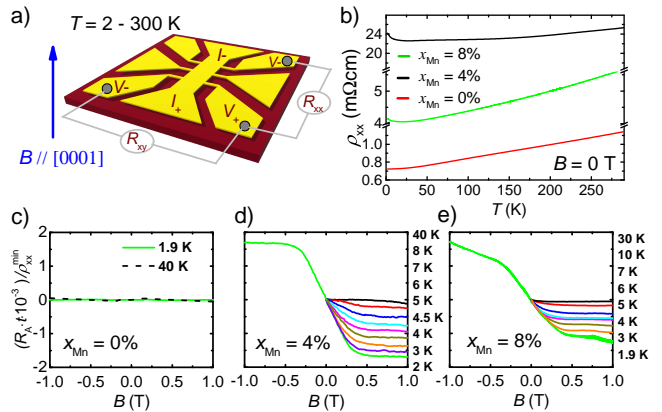


FIG. 1. (color line) (a) Hall bar measurement geometry of Mn- Bi_2Se_3 films. (b) Temperature dependence of the electrical resistivity ρ_{xx} in zero magnetic field for $x_{\text{Mn}} = 0\%$, 4%, and 8% and $t = (40 \pm 5)$ nm. (c)-(e) Respective magnetic field dependence of the anomalous Hall effect R_A .

TABLE I. Resistivities ρ_{xx}^{min} , charge carrier densities n , and carrier mobilities μ for different Mn concentrations at $T = 1.8$ K. The fitting parameter β is obtained from $\sigma_{xx}(B)$ data using Eq. 1 at 1.8 K.

	0 % Mn	4 % Mn	8 % Mn
ρ_{xx}^{min} [m Ωcm]	0.72	22.58	4.06
n [cm^{-3}]	42.7×10^{18}	1.8×10^{18}	6.2×10^{18}
μ [cm^2/Vs]	202.1	141.5	240.9
β [$\mu\text{S}/\text{T}^2$]	-0.46	-0.54	-0.21

ples with dominating donor-like Se vacancy defects [18–21].

AHE contributions R_A in Fig. 1(c-e)] are shown normalized to t/ρ_{xx}^{min} with ρ_{xx}^{min} listed in Tab. I. From the onset of the AHE we determine $T_C = (5 \pm 1)$ K and (6 ± 1) K for 4% and 8%, respectively, values close to those found by SQUID for films with $t = 500$ nm [14]. Fig. 2 summarizes the temperature dependence of the magnetoconductance $\Delta\sigma_{xx}(B) = \sigma_{xx}(B) - \sigma_{xx}(0)$ between 1.8 K and 40 K. Independently of Mn concentration, transport properties at low fields $B \leq 1$ T are dominated by WAL effects σ_{xx}^{qi} leading to cusp-shaped field dependence $\Delta\sigma_{xx}$ with convex curvature. Above 1 T, however, a transition to a concave behavior is observed, typical for Bi_2Se_3 samples beyond a critical thickness of ≈ 20 nm [22–24]. For all our samples the cusp-shaped magnetoconductivity peak at low fields is broadened with increasing temperature and finally disappears, which is a consequence of a reduced coherence length l_Φ .

For a quantitative estimation of QI effects we rely on an approximation of the full form Hikami-Larkin-Nagaoka (HLN) theory [6], where additional spin-orbit and elastic scattering as well as classical cyclotronic magnetoresistance contributions are included as a βB^2 contribution [25]:

$$\Delta\sigma_{xx} = \frac{\alpha e^2}{2\pi^2\hbar} \left[\psi \left(\frac{1}{2} + \frac{B_\Phi}{B} \right) - \ln \left(\frac{B_\Phi}{B} \right) \right] + \beta B^2 \quad (1)$$

where $\alpha \equiv \alpha_0 + \alpha_1$ generally covers both WL ($\alpha_0 > 0$) and WAL ($\alpha_1 < 0$) 2D channel contributions. B_Φ is the characteristic dephasing field, ψ the digamma function, and $B \parallel [0001]$ the external perpendicular magnetic field as shown in Fig. 1(a). The dephasing field is defined as $B_\Phi = \hbar/(4el_\Phi^2)$ and l_Φ by $l_\Phi = \sqrt{D\tau_\Phi}$, where D is the diffusion constant and τ_Φ the phase coherence time. It should be noted here that by using α as a sole fitting parameter, we assume B_Φ of WL and WAL contributions (α_0 and α_1) to be the same, which is a common assumption in the literature [26].

At low fields up to 1 T the simplified form of the HLN theory (case $\beta = 0$) proposed originally by Hikami et al. [6] is sufficient to fit the data [see Fig. 2(a), (c), and (e)]. In the full field range ($B \leq 5$ T), however, finite values $\beta < 0$ are necessary to account for the concave shape at high fields. Fits in Fig. 2(b), (d), and (f) for $x_{\text{Mn}} = 0\%$, 4% and 8%, respectively, are generated with values β listed in Tab. I. Negative values β are expected, e.g. for bulk-like cyclotronic magnetoresistance contributions [25].

We start our discussion with pure Bi_2Se_3 , where at $T = 1.8$ K and $B \leq 1$ T ($\beta = 0$) we derive values $\alpha = (-0.32 \pm 0.03)$ and $l_\Phi = (137 \pm 5)$ nm, which are comparable to those found in most previous reports [27, 28]. The fact that $\alpha < 0$ but significantly above $-\frac{1}{2}$ may be indicative of the presence of WL contribution from bulk channels [29]. Fits up to highest fields $B \leq 5$ T with $\beta = -0.46$ confirm these values within the error margins (see comparison in Supplementary Table I) and temperature dependences (see Supplementary Fig. S3) show good coincidence. This confirms that the additional fitting parameter β is reasonably independent of low-field QI contributions σ_{xx}^{qi} . When increasing the temperature, l_Φ monotonously decreases $\propto T^{-p/2}$ with $p = +(1.0 \pm 0.1)$ (see Fig. 3(a)), as expected for a Nyquist electron-scattering mechanism in 2D.

Modest magnetic doping by Mn at concentrations $x_{\text{Mn}} = 4\%$ and 8% alters QI properties (α , l_Φ) drastically as shown in Fig. 3. We stress here that for magnetic materials with small internal fields H^{int} , W(A)L effects survive as long as the magnetic length $l_m = \sqrt{\hbar/(eH^{\text{int}})}$ remains larger than the quasiparticle mean free path, which is the case for diluted magnetic materials such as (Ga,Mn)As [30].

At finite x_{Mn} , α in Fig. 3(b) is generally shifted to more negative values compared to pure Bi_2Se_3 , while temperature dependences remain weak. The corresponding temperature evolution of l_Φ in Fig. 3(a) shows a less steep increase during cooling, which can be described well by lower exponents $p = +(0.8 \pm 0.2)$ and $p = +(0.6 \pm 0.2)$ for

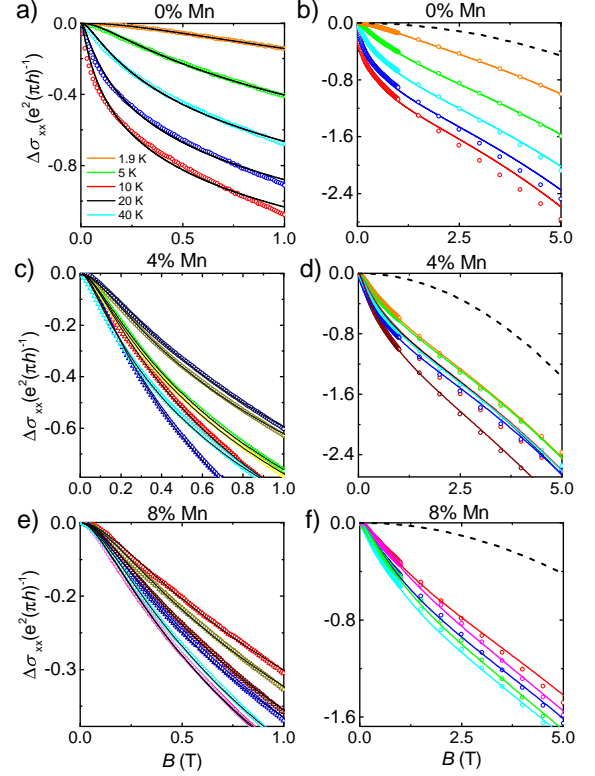


FIG. 2. (color line) Magnetic field dependence $\sigma_{xx}(B)$ for different temperatures and Mn concentrations (a,b) $x_{\text{Mn}} = 0\%$, (c,d) 4%, and (e,f) 8%. The solid lines in (a), (c), and (e) represent fits using Eq. 1 with $\beta = 0$ ($B \leq 1$ T), while (b), (d), and (f) leave β finite ($B \leq 5$ T). βB^2 contributions are plotted separately for $T = 2$ K (dashed lines).

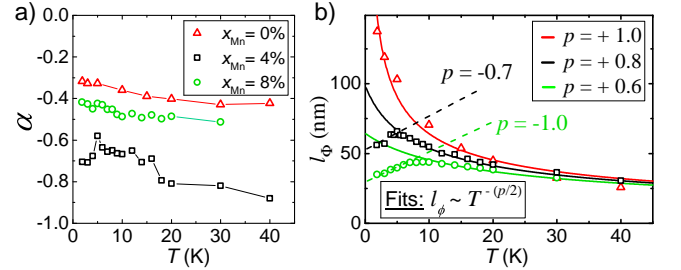


FIG. 3. (color line) Temperature dependence of (a) $\alpha(T)$ and (b) $l_\Phi(T)$ for different x_{Mn} . Values were derived from the low-field data ($B \leq 1$ T) with $\beta = 0$. l_Φ is fitted assuming $l_\Phi \propto T^{-p/2}$ for $T > T_C$ ($p > 0$, solid lines) and $T < T_C$ ($p < 0$, dashed lines).

$x_{\text{Mn}} = 4\%$ and 8%, respectively. It suggests a more efficient spin-dependent dephasing mechanism in the paramagnetic phase compared to a pure Nyquist mechanism for Mn-doped samples as we discuss below. Most interestingly, l_Φ exhibits a characteristic drop when entering the ferromagnetic phase at T_C and settles at values 30–70% of those of pure Bi_2Se_3 . It is important to mention that we checked possible influences of the build-up and satura-

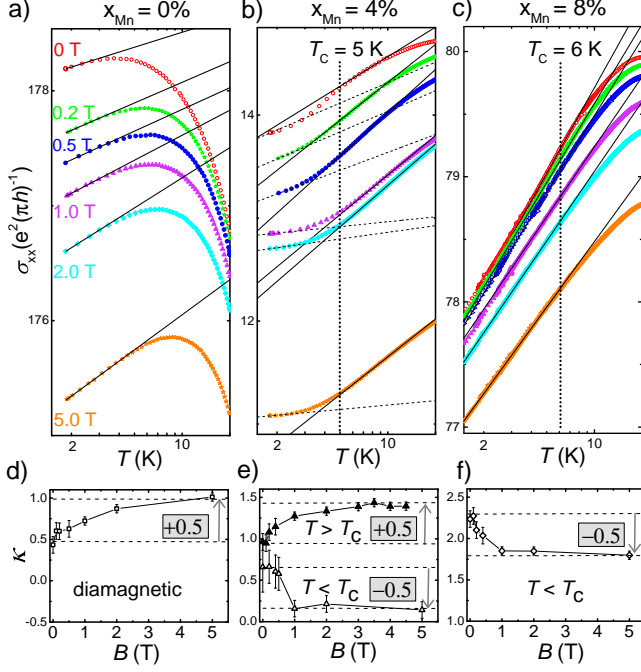


FIG. 4. (color line) (a-c) Temperature dependence of the electrical conductance in various magnetic fields on a logarithmic scale for $x_{\text{Mn}} = 0\%$, 4% and 8% Mn, respectively. Solid lines are linear fits at $T < T_E$. For 4% and 8% Mn samples T_C is indicated by a dashed vertical line. In (d)-(f) the magnetic field dependence of the slopes κ obtained from the linear fits in (a-c) are summarized.

tion of the average perpendicular magnetization $\langle M_z \rangle$ between 0 T and 0.5 T [see AHE signals in Fig. 1(d,e)] on our fitting results. Fits using HLN theory in the range between 0.5 T and 5 T lead to equivalent results for α and l_Φ within the error margins, which excludes significant influences e.g. of AMR or magnetic domain wall effects on our results.

In order to test the LS theory, QI properties described by (α, l_Φ) have to be correlated to the temperature dependence of electrical conductivities $\sigma_{xx}(T, B = \text{const})$ for different constant magnetic fields. Fig. 4 shows the presence of a logarithmic decrease $\sigma_{xx}(T) \propto \ln T$ at lowest temperatures for all samples, reminiscent of a dirty metal regime in 2D. Such a behavior was previously observed in 3D TIs in the absence of the magnetic impurities e.g. for Bi_2Te_3 [31], Bi_2Se_3 [22] and Sb_2Te_3 [12]. The logarithmic temperature dependence of the 2D conductivity with EEI corrections can be expressed by [32, 33]

$$\Delta\sigma_{xx}^{\text{EEI}}(T) = \frac{e^2}{2\pi^2\hbar} \sum_{i=0,1} (1 - \eta_H^i F_i) \ln\left(\frac{T}{T_E}\right), \quad (2)$$

where i runs over the number of independent WL and WAL 2D transport channels. F_i is the Coulomb screening factor ($0 < F_i < 1$), scaled by a factor η_H^i [15, 28, 32]. T_E is the characteristic temperature below which logarithmic EEI corrections dominate $\sigma_{xx}(T)$ [34], which is

typically in the range of $6 - 10$ K [34, 35] for Bi_2Se_3 , in line with our findings. The temperature dependence of $\Delta\sigma_{xx}^{\text{EEI}}$ in Eq. 2 can be quantified by the parameter $\kappa \equiv (\pi\hbar/e^2) \partial\sigma_{xx}/\partial\ln T$, and according to LS theory, κ for each single channel is related to its QI properties α and p via

$$\kappa = (\alpha \cdot p + 1 - \eta_H F) \quad (3)$$

in the zero magnetic field limit. For $B \gg B_\Phi$, $\kappa \simeq 1 - \eta_H F$. Thus, $\Delta\kappa(B) \simeq \alpha p$ at strong fields. It is important to note that contributions $\eta_H F$ in Eq. 3 are small: for gaps Δ with $\Delta/2E_F \leq 0.5$ (see discussion of ARPES data below) and permittivities $\epsilon_r \approx 100$ one expects $F \leq 0.1$, while η_H remains between $3/4$ and 1 for $\Delta/2E_F = 0$ and 1 , respectively. EEIs and QIs contribute via $\kappa = \kappa^{ee} + \kappa^{qi}$, where only the second term significantly depends on the ratios $\Delta/2E_F$. For one intact TSS channel with $\alpha = -0.5$ and small screening F one expects $\kappa(B = 0) \approx 0.5$ and $\kappa(B = \infty) \approx 1$. For Berry phases $\phi_{\text{Be}} = \pi$, κ thus changes by $\Delta\kappa = +0.5$, when κ^{qi} contributions are suppressed by the field.

Indeed, for pure Bi_2Se_3 we see a perfect match of κ with theory predictions for a gapless TSS. As shown in Fig. 4(a) linear fits are obtained from the logarithmic $\sigma_{xx}(T, B = \text{const})$ data at $T < T_E$, and the respective parameters $\kappa(B)$ are plotted as a function of magnetic field [Fig. 4(d)]. The value in zero magnetic field amounts to $\kappa(B = 0) \approx 0.5$, and we see a rise of κ with increasing magnetic field according to a suppression of WAL in κ^{qi} , leading to $\Delta\kappa = +0.5$ and a saturation at about $2-3$ T. The result is thus fully in line with Eq. 3 for the experimentally derived 2D Nyquist exponent $p = +1$ for pure Bi_2Se_3 . Saturation fields of $B = 3$ T in $\kappa(B)$ agree well with our estimation of l_Φ and resulting dephasing fields B_Φ . Our data thus confirms the analysis of magnetoconductance $\sigma_{xx}(B)$, that is the presence of only one single conductive gapless TSS channel [11] or - alternatively - two directly or indirectly coupled top and bottom TSSs [16, 36].

Fig. 4(b) and (c) show the respective data at $x_{\text{Mn}} = 4\%$ and 8% for a few fields with according fits for $\kappa(B)$ in the range $T < T_E$ (The full data for all fields are in the supplementary S6). For $x_{\text{Mn}} = 8\%$ again a logarithmic temperature dependence $\Delta\kappa \sim \ln T$ in Fig. 4(c) is visible in the range $T < T_E < T_C$. However, with respect to pure Bi_2Se_3 the field dependence of κ is inverted with $\Delta\kappa = -0.5$ [see Fig. 4(f)] as predicted by the theory for a gapped TSS channel. This result at first glance points towards a spectacular evidence for TRS breaking due to ferromagnetic ordering with finite $\langle M_z \rangle$. Our data for $x_{\text{Mn}} = 4\%$ with lower T_C but higher T_E would support this interpretation; above T_C we find $\Delta\kappa \approx +0.5$, while below T_C , κ turns into a decreasing behavior $\Delta\kappa \approx -0.5$.

In the following, we will show that interpreting our data as a consequence of TRS breaking is tempting but incorrect. Instead, we attribute the observed sign inver-

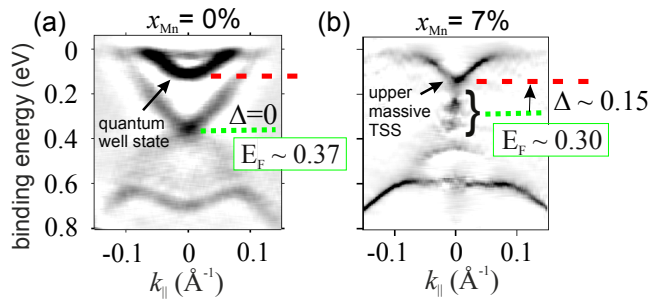


FIG. 5. (color line) (a) and (b): ARPES for $x_{\text{Mn}} = 0\%$ and 7% measured at $h\nu = 18$ eV and $T = 100$ K after 2nd derivative processing as described in the Supplementary.

sion of $\Delta\kappa$ to a large change of exponent p around T_C (recall that p describes the scaling of the dephasing time l_Φ). In order to observe a sign inversion in $\Delta\kappa$, TSSs would have to develop a sizeable gap Δ with $\Delta/2E_F \approx 1$. We keep in mind, however, that the predicted size of a purely magnetically induced gap is few meV [37, 38]. From our surface sensitive ARPES at $T > T_C$ in Fig. 5 we see strong n-doping with Fermi level shifts E_F in the range $0.3 - 0.4$ eV. It suggests $\Delta/2E_F \ll 1$ unless Δ would increase to unrealistical values. Thus, from Fig. 5(b) we expect Berry phases $\phi_{\text{Be}} = \pi[1 - (\Delta/2E_F)]$ [4] to remain close to π independent of Mn concentration and magnetic ordering processes. This is in line with our observed prevailing WAL properties with rather constant negative values α above and below T_C [Fig. 3(b)]. On the other hand, a change of sign in the temperature scaling of the dephasing time l_Φ as observed in the vicinity of T_C in Fig. 3(a) should indeed lead to an inversion in $\Delta\kappa$ according to Eq. 3. Assuming for simplicity a power law $l_\Phi \propto T^{-p/2}$ also below T_C , the data can be well described according to a transition $p = +0.8 \rightarrow -0.7$ ($p = +0.6 \rightarrow -1.0$) for $x_{\text{Mn}} = 4\%$ ($x_{\text{Mn}} = 8\%$) [see dashed lines in Fig. 3(a)], which corresponds closely to the measured inversions $\Delta\kappa = p \cdot \alpha = \pm 0.5$. This interpretation confirms the validity of the LS theory but shifts the interpretation of the observed sign inversion of $\Delta\kappa$ from a TRS breaking mechanism to a temperature-induced change (around T_C) in phase decoherent scattering behavior. Additional proof for the direct correlation between ferromagnetic ordering and transitions $p > 0 \rightarrow p < 0$ appears when reducing the sample thickness. At $t = 20$ nm thickness, ferromagnetism in 4% Mn samples is suppressed and consequently the paramagnetic QI and EEI behavior with $p = +0.8$ and $\Delta\kappa = +0.5$ is extended to lowest temperatures [see Supplementary S3(a)]. We attribute the suppression of ferromagnetism to a weakened bulk-related RKKY coupling in the reduced thickness regime, where β values collapse to 0 (Supplementary Table II) and instead Shubnikov-de Haas oscillations appear as a fingerprint for 2D-dominated transport.

Finally, we comment on microscopic mechanisms that

determine the temperature dependence of the coherence length. In the paramagnetic regime $T > T_C$ we find a remarkably good fit to data in Fig. 3(a) using $l_\Phi = a/\sqrt{T + b_x}$ where b_x is proportional to x_{Mn} (see Supplementary Fig. S6). Contrary to $l_\Phi \propto T^{-p/2}$ with p as a free fitting parameter, the former temperature dependence has a clear physical interpretation based on two uncorrelated mechanisms of inelastic scattering as explained in the Supplementary information. It suggests that Kondo-type scattering could be at work, apart from the Nyquist mechanism responsible for $l_\Phi \propto T^{-1/2}$ observed in pure Bi_2Se_3 samples. Such additional scattering mechanism, however, cannot explain the maximum in $l_\Phi(T)$ around T_C . It seems counterintuitive that perfect ferromagnetic order (or less disorder) should lead to stronger decoherence and several scenarios such as magnetic field enhanced by magnetisation or RKKY-type interactions between magnetic impurities [39] can be ruled out. We explain these in some detail in the Supplementary information along with a scattering mechanism related to spatially inhomogeneous magnetisation within the sample that gives a larger spin-flip probability at lower temperatures. Such mechanism would have the potential to explain the non-monotonous $l_\Phi(T)$ in Fig. 3(a) if it can be confirmed. Nevertheless we note that the interpretation of weak (anti)localisation measurements in the presence of spin-orbit interaction and magnetic impurities is complicated, in particular when ferromagnetism is mediated by free carriers [30] and a more detailed study of transport at low temperatures in Mn-doped Bi_2Se_3 is likely to reveal interesting physics.

This work was supported by the Czech Science Foundation Grant No. P204/14/30062S. Experiments performed in MLTL (<http://mltl.eu/>) were supported within the program of Czech Research Infrastructures (Project No. LM2011025). ARPES work was supported by VIL-LUM FONDEN via the Centre of Excellence for Dirac Materials (Grant No. 11744). VT would like to thank D. Kriegner for the lithography recipe. Scanning electron microscope assistance from K. Uhlířová is gratefully acknowledged. JW, JWa and PH acknowledge funding by the German Research Foundation via the DFG priority programme SPP1666 (grant no. WI 3097/2-2 and HO 5150/1-2). JH acknowledges the Purkyně fellowship program.

-
- [1] M. Z. Hasan and C. L. Kane, Rev. Mod. Phys. **82**, 3045 (2010).
 - [2] X.-L. Qi and S.-C. Zhang, Rev. Mod. Phys. **83**, 1057 (2011).
 - [3] J. E. Moore, Nature **464**, 194 (2010).
 - [4] H.-Z. Lu, J. Shi, and S.-Q. Shen, Phys. Rev. Lett. **107**, 076801 (2011).
 - [5] J. Honolka, A. Khajetoorians, V. Sessi, T. O. Wehling,

- S. Stepanow, J.-L. Mi, B. B. Iversen, T. Schlenk, J. Wiebe, N. B. Brookes, A. I. Lichtenstein, P. Hofmann, K. Kern, and R. Wiesendanger, *Phys. Rev. Lett.* **108**, 256811 (2012).
- [6] S. Hikami, A. I. Larkin, and Y. Nagaoka, *Progress of Theoretical Physics* **63**, 707 (1980).
- [7] D. Zhang, A. Richardella, D. W. Rench, S.-Y. Xu, A. Kandala, T. C. Flanagan, H. Beidenkopf, A. L. Yeats, B. B. Buckley, P. V. Klimov, D. D. Awschalom, A. Yazdani, P. Schiffer, M. Z. Hasan, and N. Samarth, *Phys. Rev. B* **86**, 205127 (2012).
- [8] L. Bao, W. Wang, N. Meyer, Y. Liu, C. Zhang, K. Wang, P. Ai, and F. Xiu, *Scientific Reports* **3**, 2391 EP (2013), article.
- [9] C.-Z. Chang, P. Tang, Y.-L. Wang, X. Feng, K. Li, Z. Zhang, Y. Wang, L.-L. Wang, X. Chen, C. Liu, W. Duan, K. He, X.-C. Ma, and Q.-K. Xue, *Phys. Rev. Lett.* **112**, 056801 (2014).
- [10] M. Liu, J. Zhang, C.-Z. Chang, Z. Zhang, X. Feng, K. Li, K. He, L.-l. Wang, X. Chen, X. Dai, Z. Fang, Q.-K. Xue, X. Ma, and Y. Wang, *Phys. Rev. Lett.* **108**, 036805 (2012).
- [11] H.-Z. Lu and S.-Q. Shen, *Phys. Rev. Lett.* **112**, 146601 (2014).
- [12] Y. Takagaki, A. Giussani, K. Perumal, R. Calarco, and K.-J. Friedland, *Phys. Rev. B* **86**, 125137 (2012).
- [13] L. J. Collins-McIntyre, M. D. Watson, A. A. Baker, S. L. Zhang, A. I. Coldea, S. E. Harrison, A. Pushp, A. J. Kellock, S. S. P. Parkin, G. van der Laan, and T. Hesjedal, *AIP Advances* **4**, 127136 (2014), <http://dx.doi.org/10.1063/1.4904900>.
- [14] R. Tarasenko, M. Vališka, M. Vondráček, K. Horáková, V. Tkáč, K. Carva, P. Baláž, V. Holý, G. Springholz, V. Sechovský, and J. Honolka, *Physica B: Condensed Matter* **481**, 262 (2016).
- [15] W. J. Wang, K. H. Gao, and Z. Q. Li, *Scientific Reports* **6**, 25291 EP (2016), article.
- [16] D. Kim, P. Syers, N. P. Butch, J. Paglione, and M. S. Fuhrer, *Nature Communications* **4**, 2040 EP (2013), article.
- [17] M. Brahlek, N. Koirala, M. Salehi, N. Bansal, and S. Oh, *Phys. Rev. Lett.* **113**, 026801 (2014).
- [18] Y. Liu, Y. Y. Li, D. Gilks, V. K. Lazarov, M. Weinert, and L. Li, *Phys. Rev. Lett.* **110**, 186804 (2013).
- [19] Y. Liu, Y. Y. Li, S. Rajput, D. Gilks, L. Lari, P. L. Galindo, M. Weinert, V. K. Lazarov, and L. Li, *Nat Phys* **10**, 294 (2014), letter.
- [20] S. Kim, M. Ye, K. Kuroda, Y. Yamada, E. E. Krasovskii, E. V. Chulkov, K. Miyamoto, M. Nakatake, T. Okuda, Y. Ueda, K. Shimada, H. Namatame, M. Taniguchi, and A. Kimura, *Phys. Rev. Lett.* **107**, 056803 (2011).
- [21] P. Cheng, C. Song, T. Zhang, Y. Zhang, Y. Wang, J.-F. Jia, J. Wang, Y. Wang, B.-F. Zhu, X. Chen, X. Ma, K. He, L. Wang, X. Dai, Z. Fang, X. Xie, X.-L. Qi, C.-X. Liu, S.-C. Zhang, and Q.-K. Xue, *Phys. Rev. Lett.* **105**, 076801 (2010).
- [22] J. Wang, A. M. DaSilva, C.-Z. Chang, K. He, J. K. Jain, N. Samarth, X.-C. Ma, Q.-K. Xue, and M. H. W. Chan, *Phys. Rev. B* **83**, 245438 (2011).
- [23] J. Chen, H. J. Qin, F. Yang, J. Liu, T. Guan, F. M. Qu, G. H. Zhang, J. R. Shi, X. C. Xie, C. L. Yang, K. H. Wu, Y. Q. Li, and L. Lu, *Phys. Rev. Lett.* **105**, 176602 (2010).
- [24] L. Zhang, R. Hammond, M. Dolev, M. Liu, A. Palevski, and A. Kapitulnik, *Applied Physics Letters* **101**, 153105 (2012), <http://dx.doi.org/10.1063/1.4758466>.
- [25] B. A. Assaf, T. Cardinal, P. Wei, F. Katmis, J. S. Moodera, and D. Heiman, *Applied Physics Letters* **102**, 012102 (2013), <http://dx.doi.org/10.1063/1.4773207>.
- [26] . The main reason why this assumption is commonly made is the complexity of $W(A)L$ fits when α_0 , α_1 , $B_{\Phi,0}$, and $B_{\Phi,1}$ are left as free parameters.
- [27] L. Zhang, M. Dolev, Q. I. Yang, R. H. Hammond, B. Zhou, A. Palevski, Y. Chen, and A. Kapitulnik, *Phys. Rev. B* **88**, 121103 (2013).
- [28] R. Dey, T. Pramanik, A. Roy, A. Rai, S. Guchhait, S. Sonde, H. C. P. Movva, L. Colombo, L. F. Register, and S. K. Banerjee, *Applied Physics Letters* **104**, 223111 (2014), <http://dx.doi.org/10.1063/1.4881721>.
- [29] I. Garate and L. Glazman, *Phys. Rev. B* **86**, 035422 (2012).
- [30] I. Garate, J. Sinova, T. Jungwirth, and A. H. MacDonald, *Phys. Rev. B* **79**, 155207 (2009).
- [31] H.-C. Liu, H.-Z. Lu, H.-T. He, B. Li, S.-G. Liu, Q. L. He, G. Wang, I. K. Sou, S.-Q. Shen, and J. Wang, *ACS Nano* **8**, 9616 (2014), pMID: 25184364, <http://dx.doi.org/10.1021/nn504014e>.
- [32] P. A. Lee and T. V. Ramakrishnan, *Rev. Mod. Phys.* **57**, 287 (1985).
- [33] B. L. Altshuler, A. G. Aronov, and P. A. Lee, *Phys. Rev. Lett.* **44**, 1288 (1980).
- [34] Y. Jing, S. Huang, K. Zhang, J. Wu, Y. Guo, H. Peng, Z. Liu, and H. Q. Xu, *Nanoscale* **8**, 1879 (2016).
- [35] Y. Takagaki, B. Jenichen, U. Jahn, M. Ramsteiner, and K.-J. Friedland, *Phys. Rev. B* **85**, 115314 (2012).
- [36] Z. Li, I. Garate, J. Pan, X. Wan, T. Chen, W. Ning, X. Zhang, F. Song, Y. Meng, X. Hong, X. Wang, L. Pi, X. Wang, B. Wang, S. Li, M. A. Reed, L. Glazman, and G. Wang, *Phys. Rev. B* **91**, 041401 (2015).
- [37] T. M. Schmidt, R. H. Miwa, and A. Fazzio, *Phys. Rev. B* **84**, 245418 (2011).
- [38] J. Henk, M. Flieger, I. V. Maznichenko, I. Mertig, A. Ernst, S. V. Ereemeev, and E. V. Chulkov, *Phys. Rev. Lett.* **109**, 076801 (2012).
- [39] M. G. Vavilov, L. I. Glazman, and A. I. Larkin, *Phys. Rev. B* **68**, 075119 (2003).